EVALUATION OF SPATIAL ACTIVE NOISE CANCELLATION PERFORMANCE USING SPHERICAL HARMONIC ANALYSIS

Hanchi Chen, Jihui Zhang, Prasanga N. Samarasinghe, Thushara D. Abhayapala

Research School of Engineering
College of Engineering and Computer Science
The Australian National University

ABSTRACT

This paper presents a novel metric to evaluate the performance of spatial active noise cancellation (ANC) systems. We show that the acoustic potential energy within a spherical region can be expressed by a weighed squared sum of spherical harmonic coefficients. The proposed metric allows convenient evaluation of spatial ANC performance using a spherical microphone array. In order to evaluate the effectiveness of this metric, we set up a experimental ANC system and conducted a series narrow band and wide band ANC experiments, the results show that the proposed potential energy method provides a reliable characterization of the performance of spatial ANC systems.

Index Terms— Active noise control, higher-order microphones, spherical harmonics

1. INTRODUCTION

Active noise cancellation (ANC) over space has been a key topic of research in the last two decades. Typically, ANC systems targeting spatial noise reduction are realized by Multi-Input Multi-Output (MIMO) systems [1] employing a feedforward or feedback control algorithm [2]. Most popular applications of such systems include aircraft cabin noise reduction [3] and automobile noise reduction [4, 5]. In order to successfully analyze the performance of these systems, it is important to accurately measure their noise reduction capability over space, preferably at the design stage.

At present, the performance of ANC systems is analyzed in terms of (i) sound pressure at the error microphones or (ii) recordings from a secondary microphone(s) in the cancellation region. The first approach is widely used in theory, where noise reduction performance is characterized by the average noise reduction in decibels at the error microphones [6]. The second approach is mostly used with human head shaped mannequins with 2 microphones placed at the ear locations to interpret the noise reduction levels experienced by humans [7, 8]. While both of the above methods are adequate to obtain an acceptable measure of the ANC system performance, their accuracy in terms of spatial coverage is limited due to the limited number of measurement points and the sparse nature of the spatial sampling.

In this paper, we propose an improved metric to evaluate the noise reduction in spatial regions. It is formulated in terms of the spherical harmonic decomposition of soundfields and requires the measurements from a secondary microphone array distributed over a spherical surface, preferably enclosing the center of the region of interest. The spatial metric is defined as the acoustic potential energy inside a spherical region, and we formulate it in terms of the aforementioned microphone array recordings. A similar spatial metric was introduced in [9] for rectangular enclosures, where the acoustic potential energy was described in terms of room modes. However, the results were limited to simulations and the extraction of room modes is difficult in practical applications where the natural modes of a room depends greatly on the geometry of the room.

The proposed potential energy method calculates the average noise level in the entire spatial region, therefore there is no need to take multiple samplings of the control region, which simplifies the process of ANC performance evaluation. Compared to [9], our method represents the potential noise using spherical harmonic coefficients rather than room modes, which can be conveniently captured by spherical microphone arrays. The main advantage of this approach is its applicability to any arbitrary enclosure and its independence from the ANC system of use. Therefore our method is particularly suitable for environments with irregular geometry and a fixed control region with moderate size, such vehicle and aircraft cabins.

In order to demonstrate the usefulness of the proposed metric, we carried out experiments using a MIMO ANC system with 5-error microphones and 2-secondary loudspeakers attempting to cancel a noise field caused by a single primary source. The microphone recordings required to evaluate the spatial performance metric were obtained using a 32 channel Eigenmike [10].

2. EVALUATION OF THE SPATIAL NOISE REDUCTION BY A MIMO ANC SYSTEM

Irrespective of the ANC algorithm of use, typical applications target noise reduction over a continuous spatial region. In this section, we mathematically formulate a spatial metric to evaluate the noise reduction experienced over the region of interest. We define this metric as the acoustic potential energy within a spherical region.

2.1. Spherical harmonic decomposition of a sound field

The sound pressure at any arbitrary point within a homogeneous medium is described by the Helmholtz wave equation in the frequency domain. A solution to this wave equation can be derived in terms of a set of spatial basis functions called the *spherical harmonics*. For a source free incident soundfield, this parameterization is of the form [11]

$$P(r,\vartheta,\varphi,k)=\sum_{v=0}^{\infty}\sum_{\mu=-v}^{v}\alpha_{v\mu}(k)j_v(kr)Y_{v\mu}(\vartheta,\varphi), \qquad (1)$$

This work is supported by Australian Research Council (ARC) Discovery Projects funding scheme (project no. DP140103412).

where (r, ϑ, φ) is the observation point with respect to the origin, $k = 2\pi f/c$ is the wave number, f is the frequency, c is the wave propagation speed, $\alpha_{v\mu}(k)$ are the frequency-domain spherical harmonic coefficients, $j_v(kr)$ are the spherical Bessel functions of order v, and $Y_{v\mu}(\vartheta, \varphi)$ are the spherical harmonics of order v and degree μ. The spatial basis functions $Y_{v\mu}(\vartheta, \varphi)$ have the orthogonal property

$$\int_0^{\pi} \int_0^{2\pi} Y_{v\mu}(\vartheta, \varphi) Y_{v'\mu'}(\vartheta, \varphi)^* \sin(\vartheta) d\vartheta d\varphi = \delta_{v-v',\mu-\mu'}, \quad (2)$$

where $\delta_{v,\mu}$ is the two dimensional Dirac Delta function.

Due to the inherent properties of the Bessel function, the infinite summation in (1) can be truncated at $V = \lceil kR \rceil$[12], where R is the furthest observation distance of interest. Given that the sound-field coefficients $\alpha_{v\mu}(k)$ are independent of the observation point, the aforementioned truncation states that any arbitrary incident field over spherical region of radius R can be completely characterized by a finite set of coefficients $\alpha_{v\mu}(k)$. Therefore, in an ANC scenario, the sound field coefficients of the reduced noise field carry most information about the global noise reduction achieved by the ANC system. Methods to compute these coefficients using a spherical microphone array with open / rigid body are detailed in [13] and [14], respectively.

2.2. Calculation of the acoustic potential energy

The acoustic potential energy of the enclosure is a sensible measure, that when minimized, will result in the global reduction of sound. In a spherical region of interest, it can be represented by

$$E_p(k) = \frac{1}{4\rho_0 c^2} \int_S |P(r, \vartheta, \varphi)|^2 dS, \quad (3)$$

where $\int_S dS = \int_0^R \int_0^{\pi} \int_0^{2\pi} r^2 dr \sin(\vartheta) d\vartheta d\varphi$ denote the integral over a sphere. Using (1), we can decompose the integral of sound energy as [15]

$$\begin{aligned} &\int_S |P(r, \vartheta, \varphi)|^2 dS \\ &= \int_0^R \int_0^{\pi} \int_0^{2\pi} P(r, \vartheta, \varphi) P^*(r, \vartheta, \varphi) r^2 dr \sin(\vartheta) d\vartheta d\varphi \quad (4) \\ &= \sum_{n,m} \alpha_{nm} \alpha_{nm}^* \int_0^R j_n^2(kr) r^2 dr, \quad (5) \end{aligned}$$

where the orthogonal property of the spherical harmonics (2) was used. Therefore (5) can be expressed using the spherical harmonic coefficients as

$$E_p(k) = \frac{1}{4\rho_0 c^2} \sum_{v,\mu} |\alpha_{v\mu}(k) W_v(k)|^2, \quad (6)$$

where ρ_0 denotes the density of the media and c is the speed of sound.

$$W_v(k) = \Big(\int_0^R j_v(kr)^2 r^2 dr \Big)^{1/2}. \quad (7)$$

The above result shows that the acoustic potential energy within a spherical region is given by a sum of squared spherical harmonic coefficients with the weighting $W_v(k)$. Therefore, as soon as the spherical harmonic coefficients representing the noise field is obtained using a suitable microphone array, the acoustic potential energy can be easily computed using (6). The weights $W_v(k)$ can be pre-calculated for each frequency and each active spherical harmonic order, therefore it does not incur additional computational complexity if the potential energy is to be monitored in real time.

3. EXPERIMENT SETUP

3.1. ANC algorithm

In order to investigate the performance of the proposed spatial noise level measurement criteria, a MIMO ANC system is set up inside lab environment.

The commonly used FxLMS algorithm is implemented, and the block diagram of the ANC system is shown in Fig.1. In the figure, $\boldsymbol{U}$ is the primary path. $\boldsymbol{H}$ and $\hat{\boldsymbol{H}}$ represent the secondary path from the adaptive filters to the error microphones and the secondary path model, respectively.

The reference input signals are $x_i(n), i = 1, \ldots, I$ and the instantaneous error microphone measurements are $e_m(n), m = 1, \ldots, M$. The error signals can be written as $e_m(n) = d_m(n) + y'_m(n)$, where $y'_m(n) = y_z(n) * H_{zm}(n)$, where $H_{zm}(n)$ denotes the impulse response from the zth secondary source to the mth error microphone, $y_z(n)$ are the loudspeaker driving signals, and $*$ denotes linear convolution. The zth secondary speaker driving signal is generated as

$$y_z(n) = \sum_{i=1}^{I} \boldsymbol{w}_{iz}^T(n) \boldsymbol{x}_i(n), \text{for } z = 1, 2, \ldots, Z, \quad (8)$$

where $\boldsymbol{w}_{iz}(n) = [w_{iz,0}(n), w_{iz,1}(n), \ldots, w_{iz,L-1}(n)]^T$ are the adaptive filter coefficients in the nth iteration, $\boldsymbol{x}_{iz}(n) = [x_{i,0}(n), x_{i,1}(n), \ldots, x_{i,L-1}(n)]^T$, and L is the length of the FIR adaptive filters. The update equation for $\boldsymbol{w}_{iz}(n)$ is given by

$$\boldsymbol{w}_{iz}(n+1) = \boldsymbol{w}_{iz}(n) - \lambda \sum_{m=1}^{M} \boldsymbol{x}'_{izm}(n) e_m(n), \quad (9)$$

where λ is the step size, $\boldsymbol{x}'_{izm}(n) = [x'_{izm}(n), \ldots, x'_{izm}(n-L+1)]^T$ is a vector of filtered reference signals, and $x'_{izm}(n) = x_i(n) * \hat{H}_{zm}(n)$.

In our implementation, $I = 1, Z = 2, M = 5$.

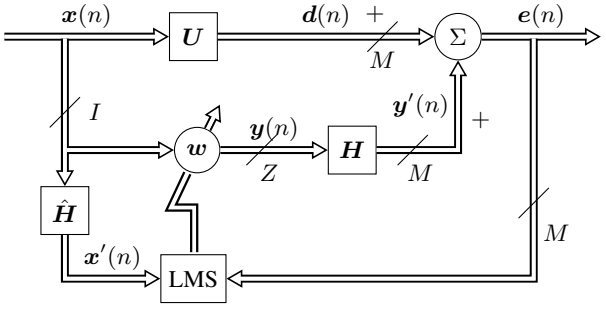

Fig. 1. Block diagram of the multiple-channel feedforward ANC system.

3.2. Hardware Configuration

The hardware configuration of the system is shown in Fig. 2, where the control region is defined as a spherical area with 0.1 m radius,

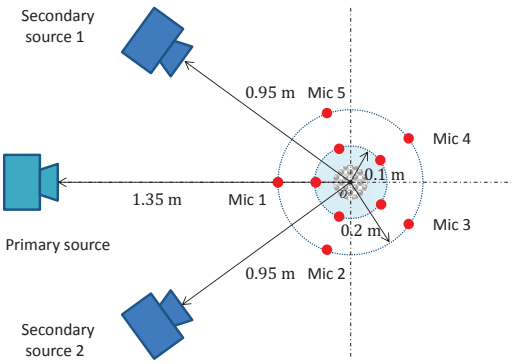

Fig. 2. Loudspeaker and microphone placement for the experiment.

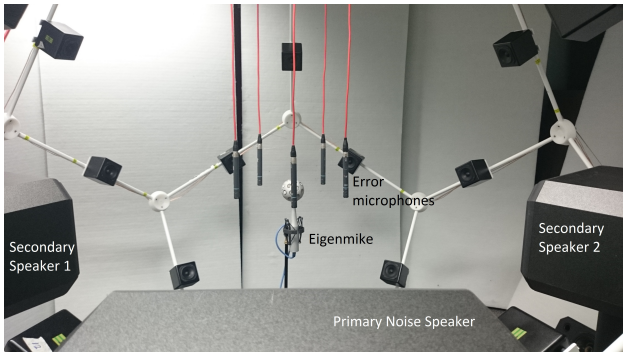

Fig. 3. Picture of the experiment setup, the small loudspeakers in the background are not used in the experiment.

which approximately covers the size of a human head. Five AKG CK92 omnidirectional microphones are placed evenly on the horizontal plane boundary of the region, which act as the error sensors.

In order to investigate the differences in ANC performance due to different error microphone setups, we vary the radius of the error microphone array between 10 cm and 20 cm, and conduct experiments for both radii setups. Further more, we also investigate the scenario where only two of the error microphones are used for ANC, in this configuration, only "Mic 2" and "Mic 5" shown in Fig. 2 are active.

Three TANNOY 600 loudspeakers are used as the primary and secondary sources. The two secondary speakers are placed on either side of the primary source, forming an angle of 72 degrees. The error microphone signals are transmitted to a PC, which performs the adaptive ANC algorithm and generates the secondary loudspeaker driving signals in real time. Since the focus of this experiment is not on the performance of the MIMO ANC algorithm itself, the reference signal is obtained directly from the electronic signal path of the primary source, rather than using a separate reference microphone. This eliminates the feedback signal path from the secondary sources to the reference sensor which may affect the ANC performance.

An Eigenmike is placed at the center to monitor the noise field within the control region. Although the Eigenmike is capable of capturing spatial sounds up to 4 th order at 4 kHz, we only focus on the lower frequency sounds (up to 800 Hz and 1st order). This is because at higher frequencies, the second order spherical harmonics begins to have a higher contribution towards the sound energy close to the boundary of control region, but the Eigenmike is unable to capture the second order sound field at that frequency, due to its smaller radius (4.2 cm) compared to the control region.

During operation, a separate computer is used to process the audio signal recorded by the Eigenmike and calculate the potential energy simultaneously. The Eigenmike is not involved in the signal path of the ANC system in any way.

Both narrow and wide band signals are used as the primary noise for the experiments. The narrow band signals are sine waves of frequencies $100-800$ Hz; the wide band signal is generated by filtering a in-car noise recording through a $100-800$ Hz bandpass filter.

For narrow band experiments, a sine wave is played through the primary speaker, then we calculate the average sound energy recorded by each error microphone with and without ANC, and calculate the attenuation of the noise energy due to ANC. The attenuation of the average sound energy within the control region is measured in the same way.

For wide band experiments, we play the wide band noise and record a section of signal from the error microphones as well as the Eigenmike while the ANC system is not active, then repeat the recording with ANC active and fully converged. We then calculate the average frequency spectrum of each recorded section. The playback and recordings are synchronized such that the same section of noise signal is recorded each time.

4. RESULT ANALYSIS

4.1. Effect of microphone array radius

In order to investigate the effect of microphone array radius on the performance of the ANC system at different frequencies, as well as the differences between the potential energy criteria and microphone pressure criteria, we conduct the narrow band ANC experiments for microphone array radius $r = 10$ cm and $r = 20$ cm, utilizing all 5 microphones. The energy attenuation of both potential energy and microphone received signal are shown in Fig. 4 (a).

It can be seen from Fig. 4 (a) that for all configurations, overall the noise attenuation becomes smaller as the frequency increases. A potential energy attenuation of over -10 dB can be achieved for frequencies up to 450 Hz if the microphones are placed on the boundary of the control region; when the microphones are placed further away, the attenuations are worse by $5-10$ dB for frequencies above 300 Hz. This result is intuitive because when the microphones are placed further away, the correlation between the sound pressure inside the control region and the sound pressure at microphone positions becomes smaller, and this is especially true for higher frequencies, where the wavelength is shorter. However, it can be seen that at very low frequencies (below 200) Hz, both radii result in very similar ANC performance in terms of potential energy attenuation.

Comparing the curves corresponding to microphone signal attenuation with those corresponding to potential energy attenuation, it can be found that when the microphones are placed at the boundary of the region, the microphone signals are a good indication of the potential energy inside the region; when the microphones are placed further away, however, the microphone signal attenuations become much smaller than the noise attenuation observed inside the region. In this case, the microphone signals are no longer a good indication of the ANC systems' performance.

4.2. Effect of microphone number

The effect of the number of error microphones is also investigated. For this purpose, we repeat the narrow band experiments with only

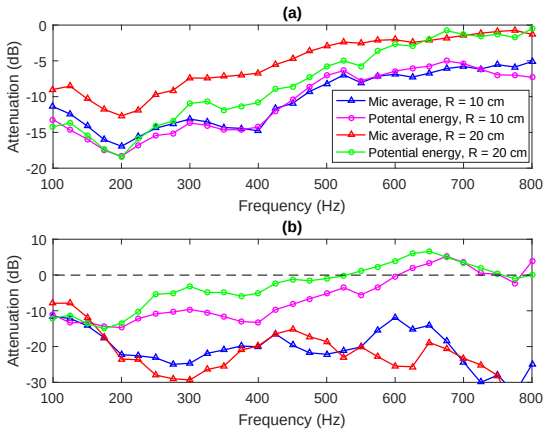

Fig. 4. Average narrow band noise energy attenuation at control region and microphone locations using 5 error microphones (a) and 2 error microphones (b). Legend of (b) is the same as (a).

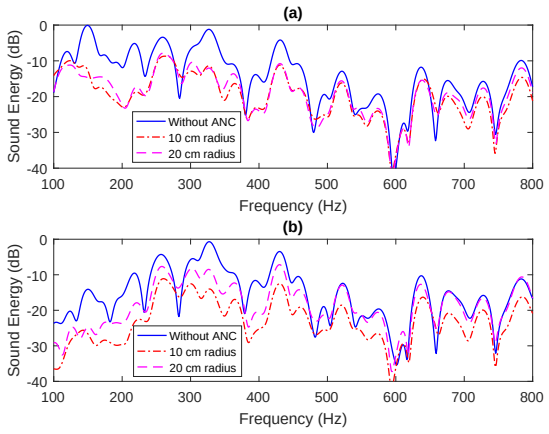

Fig. 5. Spectrum of potential energy at control region (a) and microphone locations (b) using wide band noise signal.

two error microphones active, and the noise attenuation results are shown in Fig. 4 (b). From this figure, it can be observed that both the microphone signal attenuations and the potential energy attenuations become very different from the case where 5 microphones are used. In particular, the microphone signals can achieve more than -10 dB attenuation for all frequencies, and the attenuation does not decay with increased frequency; on the other hand, the potential energy attenuation is significantly worse compared to the 5 channel case, and the value even became positive (higher noise level with ANC active) at some higher frequencies.

The cause of this phenomenon is that the number of error microphones is equal to the number of secondary sources, therefore a solution always exists to significantly reduce the sound pressure at the microphone positions, but often at the cost of very high secondary source driving signals. Since the two microphones cannot provide a complete coverage of the control region, the potential energy inside the region becomes less controllable compared to the 5 channel case, and in some extreme cases, this results in positive attenuation inside the region. In this case, the microphone signals are not a good indication of the ANC performance inside the control region, except at very low frequencies (below 150 Hz), as can be seen in Fig. 4 (b).

4.3. Wide band performance

In order to investigate the system's wide band performance, we compute the average spectrum of the microphone signals with and without ANC, as well as the spectrum of observed potential energy within the control region. All five error microphones are used in this experiment. The spectrums are shown in Fig. 5, where Fig. 5 (a) plots the potential energy, and Fig. 5 (b) plots the spectrum of microphone signals. The difference of spectrums at low frequency between Fig. 5 (a) and (b) is due to the high pass filters in the error microphones' amplification circuitry. From Fig. 5 (a) it can be seen that overall the wide band ANC performance agrees with the corresponding narrow band results shown in Fig. 4 (a), where an attenuation of -10 dB and more can be achieved for most frequencies below 400 Hz, while at higher frequencies, the attenuation gradually reduces to -3 to -5 dB. Comparing the curves corresponding to 10 cm and 20 cm microphone array radius, it can be seen that the low frequency ANC performance of the two configurations are very similar, with the 10 cm configuration being superior at certain frequency ranges. At higher frequencies, the 10 cm configuration yields consistently better attenuation than the 20 cm configuration, which also agrees with Fig. 4 (a), although the attenuation is slight worse for the 10 cm radius case.

In the case of Fig. 5 (b), the attenuation observed at microphone positions differs greatly for the two radius configurations. For 10 cm radius, the attenuation is greater than 5 dB for nearly all frequencies between $100 - 800$ Hz, while for the 20 cm setup, the attenuation becomes negligible above 475 Hz. Up on closer observation, it can be seen that the microphone attenuation at 10 cm radius is -2 to -3 dB greater than that of the potential energy inside the control region. Therefore, neither of the two microphone position configurations truthfully reflect the ANC performance within the control region, although the result is more accurate when the microphones are placed closer to the control region. We note that in a real-life environment, the noise field is likely to be more complicated, in which case the ANC performance will be worse than the results shown above.

Overall, it can be seen that the error microphone signals cannot be used to reliably measure the noise attenuation inside the control region, especially when the number of error microphones is small, or when the microphones are not place close to the control region. On the other hand, using the proposed method, we can use a spherical microphone array placed in the center of the region to conveniently and reliably monitor the potential energy within the region.

5. CONCLUSION

In this work, a novel metric to evaluate the performance of ANC systems is proposed. We use a spherical harmonics based algorithm to monitor the noise field, and calculate the acoustic potential energy within a spherical control region using a weighed squared sum of spherical harmonic coefficients. Through a series of experiments using a MIMO ANC system, we show that the proposed method provides a more robust and accurate measurement of spatial ANC performance compared to the existing method based on error microphone signals energies for measuring the noise level within a 0.1 m spherical region. It can be utilised in practical performance evaluation for the in car noise cancellation systems.

6. REFERENCES

[1] Y. Kajikawa, W. S. Gan, and S. M. Kuo, "Recent advances on active noise control: Open issues and innovative applications," *APSIPA Transactions on Signal and Information Processing*, vol. 1, pp. 21, Apr 2012.

[2] S. M. Kuo and D. R. Morgan, "Active noise control: A tutorial review," *Proceedings of the IEEE*, vol. 87, no. 6, pp. 943–973, Jun 1999.

[3] S.J. Elliot, P.A. Nelson, I.M. Stothers, and C.C. Boucher, "In-flight experiments on the active control of propeller-induced cabin noise," *Journal of Sound and Vibration*, vol. 140, no. 2, pp. 219–238, Jul 1990.

[4] H. Sano, T. Inoue, A. Takahashi, K. Terai, and Y. Nakamura, "Active control system for low-frequency road noise combined with an audio system," *IEEE Transactions on Speech Audio Processing*, vol. 9, no. 7, pp. 755–763, Oct 2001.

[5] J. Cheer, *Active control of the acoustic environment in an automobile cabin*, Ph.D. thesis, University of Southampton, 2012.

[6] S. C. Douglas, "Fast implementations of the filtered-X LMS and LMS algorithms for multichannel active noise control," *IEEE Transactions on Speech and Audio Processing*, vol. 7, no. 4, pp. 454–465, Jul 1999.

[7] M. de Diego, A. Gonzalez, M. Ferrer, and G. Pinero, "An adaptive algorithms comparison for real multichannel active noise control," in *12th European Signal Processing Conference*, Vienna, Austria, Sep 2004, pp. 925–928.

[8] M. de Diego, A. Gonzalez, M. Ferrer, and G. Pinero, "Multichannel active noise control system for local spectral reshaping of multifrequency noise," *Journal of Sound and Vibration*, vol. 274, no. 1-2, pp. 249–271, Jul 2004.

[9] A. Montazeri, J. Poshtan, and M. H. Kahaei, "Analysis of the global reduction of broadband noise in a telephone kiosk using a MIMO modal ANC system," *International Journal of Engineering Science*, vol. 45, no. 2-8, pp. 679–697, 2007.

[10] "em32 eigenmike microphone array release notes," www.mhacoustics.com/sites/default/files/ReleaseNotes.pdf, 2013.

[11] E. G. Williams, *Fourier Acoustics: Sound Radiation and Near field Acoustical Holography*, USA: Academic, 1999.

[12] R.A. Kennedy, P. Sadeghi, T.D. Abhayapala, and H.M. Jones, "Intrinsic limits of dimensionality and richness in random multipath fields," *IEEE Transactions on Signal Processing*, vol. 55, no. 6, pp. 2542–2556, Jun 2007.

[13] T. D. Abhayapala and D. B. Ward, "Theory and design of high order sound field microphones using spherical microphone array," in *IEEE International Conference on Acoustics, Speech, and Signal Processing (ICASSP)*, Orlando, Florida, USA, May 2002, vol. 2, pp. II–1949–II–1952.

[14] J. Meyer and G. Elko, "A highly scalable spherical microphone array based on an orthonormal decomposition of the soundfield," in *IEEE International Conference on Acoustics, Speech, and Signal Processing (ICASSP)*, Orlando, Florida, USA, May 2002, vol. 2, pp. II–1781–II–1784.

[15] H. Chen, P. Samarasinghe, T. D. Abhayapala, and W. Zhang, "Spatial noise cancellation inside cars: Performance analysis and experimental results," in *2015 IEEE Workshop on Applications of Signal Processing to Audio and Acoustics (WASPAA)*, New Paltz, New York, USA, Oct 2015, pp. 1–5.